Performance Analysis of Full-Duplex Spatial Modulation Systems With Transmit Antenna Selection

Le Van Nguyen, Ba Cao Nguyen, Xuan Nam Tran
Advanced Wireless Communications Group
Le Quy Don Technical University, Hanoi, Vietnam
(e-mail: vannl@mta.edu.vn, bacao.sqtt@gmail.com, namtx@mta.edu.vn)

***Abstract*—In this paper, we analyze performance of the bidirectional Full Duplex (FD) Spatial Modulation (SM) systems using Transmit Antenna Selection (TAS), called FD-SM-TAS, in the presence of Residual Self-Interference (RSI) due to imperfect Self-Interference Cancellation (SIC). Based on mathematical calculation, the exact Outage Probability (OP) expression of the FD-SM-TAS system is derived. Besides, OP performance of the FD-SM system with and without TAS is compared to confirm the efficacy of TAS. The derived expression can be used for Half Duplex (HD) systems with and without TAS when setting the value of RSI to zero. Impacts of data transmission rate and RSI on the system performance are also investigated and compared with those of the HD-SM system. Finally, the analytical results are validated by Monte Carlo simulation.**

***Index Terms*—Full duplex (FD), spatial modulation (SM), transmit antenna selection (TAS), outage probability (OP)**

I. Introduction

Full Duplex (FD) communication allows simultaneous transmission and reception at the same frequency and same time slot, thus theoretically doubling the spectral efficiency compared with Half Duplex (HD) communications [1], [2]. However, FD transmission produces high-power Self-Interference (SI), i.e. the interference leaking from the transmitter to the receiver within a transceiver, which reduces the capacity of FD systems [3]–[9]. Significant efforts have been made in various fields such as signal processing and antenna design for effectively suppressing this SI. However, these Self-Interference Cancellation (SIC) techniques are not capable of fully mitigating SI but can only reduce it to an acceptable level at the receiver [10], making it possible to implement the FD concept in practical systems.

Meanwhile, Spatial Modulation (SM) is an effective technique to increase the spectral efficiency of a multiple-input multiple-output (MIMO) system by using antenna indices as a means of information bearing. In an SM system, only one antenna is activated according to the incoming data bits to transmit an $M-$PSK/QAM symbol. The SM system uses only a single antenna for transmitting and thus can avoid Inter Channel Interference (ICI) and antenna synchronization problems [11], [12] as in the conventional MIMO system. It is considered a low-complexity, yet energy-efficient MIMO transmission technique. There are many efforts to combine FD transmission and SM in the literature [2], [13]–[15]. In [2], an FD-SM system is proposed for a 2×2 MIMO system. Closed-form expressions of the Outage Probability (OP) and ergodic capacity were compared with those of the conventional FD and HD systems. The authors in [13] considered a combined SM and FD system in the two-way relay channel. The upper bound on the Average Bit Error Probability (ABEP) was derived and the exact SNR threshold to select the FD/HD mode was determined. Performance of the FD-SM system was investigated in [14]. The upper bounds for the Bit Error Rate (BER) expressions of the FD-SM system were derived for both PSK and QAM constellations in the presence of imperfect channel state information. The work in [15] evaluated performance of a SM-aid FD relaying protocol, in which the direct link between the source and destination node was exploited. The average Symbol Error Probability (ASEP) of this system was derived under the impact of Residual Self-Interference (RSI). These previous works have demonstrated that FD-SM is a spectrum-efficient and low complexity system with a certain level of performance penalty because of the RSI due to imperfect SIC at the receiver.

In order to overcome the impact of such RSI, a simple yet effective solution is to use Transmit Antenna Selection (TAS). Using this TAS solution, the transmitter selects S out of N_t transmitting antennas with higher channel gains to implement SM. It was demonstrated that an SM system with TAS attains better performance than the one without TAS [16]–[18]. Antenna selection was also introduced in the FD MIMO system in [19]–[21]. It was shown that performance of the FD MIMO system could be improved significantly by using transceiver antenna selection.

However, to the best of our knowledge, no prior work has considered the FD-SM system with TAS. Motivated by this open problem, in this paper, we intent to conduct a detailed analysis on the performance of the FD-SM system with TAS (referred to for short as FD-SM-TAS). The main contributions of the paper can be summarized as follows:

- We investigate performance of the FD-SM-TAS system under the impact of RSI due to imperfect SIC at two transceivers and derive its exact OP expression. The advantage of TAS is also analyzed to see its improvement against the case without TAS.

- Applying the obtained OP expression for the FD-SM-TAS system to a half-duplex SM (HD-SM) system, we analyze the performance degradation of using the FD mode against the HD mode.

The rest of the paper is organized as follows. Section II presents the system model of the considered FD-SM-TAS system. The exact OP expression of the considered system under the Rayleigh fading channel is derived in Section III. Numerical results and performance evaluations are provided in Section IV. Finally, Section V draws the conclusion of the paper.

978-1-7281-2392-9/19/$31.00 ©2019 IEEE

II. System Model

Fig. 1. depicts the block diagram of the considered FD-SM-TAS system. The information is transferred between two communication transceivers, i.e. A and B. Both A and B are MIMO transceivers which operate at the FD mode. We consider the case that A and B use separate antennas for transmission and reception. Although A and B can employ shared-antennas for both transmit and receive modes simultaneously, using separate antennas has been proved to obtain better SI suppression [22], [23]. Besides, A and B respectively have $N_t^{\mathrm{A}}, N_t^{\mathrm{B}}$ antennas for transmitting and N_r^{A}, N_r^{B} antennas for receiving. As shown in Fig. 1, the FD operation at each transceiver results in SI which distorts the desired receive signal.

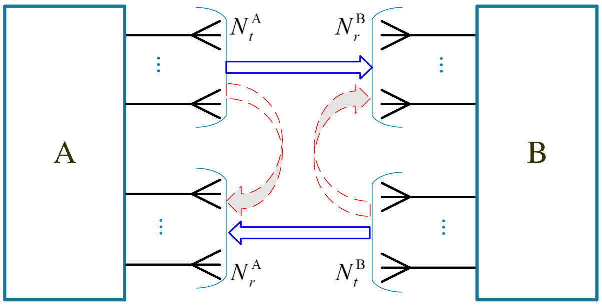

Figure 1. Block diagram of FD-SM system with self-interference.

At time slot t, the received signals at A and B are respectively given by

$$\mathbf{y}_{\mathrm{A}}(t) = \sqrt{P_{\mathrm{B}}}\mathbf{h}_j^{\mathrm{A}} x_j(t) + \sqrt{P_{\mathrm{A}}}\mathbf{h}_i^{\mathrm{A}} x_i(t) + \mathbf{z}_{\mathrm{A}}(t), \quad (1)$$

$$\mathbf{y}_{\mathrm{B}}(t) = \sqrt{P_{\mathrm{A}}}\mathbf{h}_i^{\mathrm{B}} x_i(t) + \sqrt{P_{\mathrm{B}}}\mathbf{h}_j^{\mathrm{B}} x_j(t) + \mathbf{z}_{\mathrm{B}}(t), \quad (2)$$

where $x_i(t)$ and $x_j(t)$ are transmitted signals from the i-th activated antenna of A and the j-th activated antenna of B, respectively, where $i = 1, 2, ..., N_t^{\mathrm{A}}$ and $j = 1, 2, ..., N_t^{\mathrm{B}}$; P_{A} and P_{B} are the average transmit powers of A and B, respectively; $\mathbf{h}_i^{\mathrm{B}} = [h_{i1}, h_{i2}, \ldots, h_{iN_r^{\mathrm{B}}}]$ and $\mathbf{h}_j^{\mathrm{A}} = [h_{j1}, h_{j2}, \ldots, h_{jN_r^{\mathrm{A}}}]$ denote respectively the channel vectors whose elements are the channel gains from the i-th transmit antenna of A to N_r^{B} receive antennas of B and from the j-th transmit antenna of B to N_r^{A} receive antennas of A; $\mathbf{h}_i^{\mathrm{A}}$ and $\mathbf{h}_j^{\mathrm{B}}$ are respectively the SI channel vectors which contain the SI coefficients from the i-th transmit antenna of A to its N_r^{A} receive antennas and from the j-th transmit antenna of B to its N_r^{B} receive antennas; $\mathbf{z}_{\mathrm{A}}(t)$ and $\mathbf{z}_{\mathrm{B}}(t)$ are, respectively, the Additive White Gaussian Noise (AWGN) vectors at A and B. Each element of the noise vectors is modeled by a complex normal random variable with zero-mean and variance of σ^2, i.e. $\mathbf{z}_{\mathrm{A}} \sim \mathcal{CN}(0, \sigma_{\mathrm{A}}^2)$ and $\mathbf{z}_{\mathrm{B}} \sim \mathcal{CN}(0, \sigma_{\mathrm{B}}^2)$.

Because the separations between transmit antennas to receive antennas of each transceiver are often very small compared to the distance between the two transceivers, the SI power at the receiver are actually stronger than the desired signal power. Therefore, SIC techniques must be used to reduce the SI power to guarantee the signal quality for detecting the desired signal. In this paper, we assume that A and B use a combined SIC technique in all three domains, i.e. antenna, analog and digital domain. Under this assumption, RSI at each transceiver A and B, denoted by $\mathbf{r}_{\mathrm{SI_A}}$ and $\mathbf{r}_{\mathrm{SI_B}}$ respectively, can be modeled using complex Gaussian distributed random variables [3], [4], [24] with zero-mean and variance of σ_{RSI}^2, i.e. $\sigma_{\mathrm{RSI_A}}^2 = \tilde{\Omega}_{\mathrm{A}} P_{\mathrm{A}}$ and $\sigma_{\mathrm{RSI_B}}^2 = \tilde{\Omega}_{\mathrm{B}} P_{\mathrm{B}}$, where $\tilde{\Omega}_{\mathrm{A}}$ and $\tilde{\Omega}_{\mathrm{B}}$ indicate the SIC capability at A and B, respectively.

Therefore, the received signals at A and B after SIC is given by

$$\mathbf{y}_{\mathrm{A}}(t) = \sqrt{P_{\mathrm{B}}}\mathbf{h}_j^{\mathrm{A}} x_j(t) + \mathbf{r}_{\mathrm{SI_A}}(t) + \mathbf{z}_{\mathrm{A}}(t), \quad (3)$$

$$\mathbf{y}_{\mathrm{B}}(t) = \sqrt{P_{\mathrm{A}}}\mathbf{h}_i^{\mathrm{B}} x_i(t) + \mathbf{r}_{\mathrm{SI_B}}(t) + \mathbf{z}_{\mathrm{B}}(t). \quad (4)$$

In the SM-MIMO system, only one antenna is activated from N_t^{A} transmit antennas of A and one from N_t^{B} transmit antennas of B for transmitting signal symbols according to the incoming data bits in each transceiver. In the case of TAS, at transceiver A, a set of S_{A} transmit antennas are selected from N_t^{A} transmit antennas while at transceiver B, a set of S_{B} transmit antennas are selected from N_t^{B} transmit antennas. It is noticed that S_{A} and S_{B} are subject to $S_{\mathrm{A}} \le N_t^{\mathrm{A}}, S_{\mathrm{A}} = 2^m$, and $S_{\mathrm{B}} \le N_t^{\mathrm{B}}, S_{\mathrm{B}} = 2^n$ with m and n are positive integers. The set of S_{A} and S_{B} are selected to maximize the total received signal power. For example, when the norms of the channel coefficients satisfy

$$\|\mathbf{h}_1^{\mathrm{B}}\|^2 \ge \|\mathbf{h}_2^{\mathrm{B}}\|^2 \ge \|\mathbf{h}_3^{\mathrm{B}}\|^2 \ge ... \ge \|\mathbf{h}_{N_t^{\mathrm{A}}}^{\mathrm{B}}\|^2, \quad (5)$$

and $S_{\mathrm{A}} = 2$, we have the set S_{A} as

$$S_{\mathrm{A}} = \{\|\mathbf{h}_1^{\mathrm{B}}\|^2, \|\mathbf{h}_2^{\mathrm{B}}\|^2\}. \quad (6)$$

From this selected set, either the first or second antenna of A is activated for transmitting according to the incoming data bits.

Using (3) and (4), the signal-to-interference-plus-noise ratios (SINR) at transceiver A and B (denoted by γ_{A} and γ_{B} respectively) are calculated as follows

$$\gamma_{\mathrm{A}} = \frac{\|\mathbf{h}_j^{\mathrm{A}}\|^2 P_{\mathrm{B}}}{\sigma_{\mathrm{RSI_A}}^2 + \sigma_{\mathrm{A}}^2} = \|\mathbf{h}_j^{\mathrm{A}}\|^2 \bar{\gamma}_{\mathrm{A}}, \quad (7)$$

$$\gamma_{\mathrm{B}} = \frac{\|\mathbf{h}_i^{\mathrm{B}}\|^2 P_{\mathrm{A}}}{\sigma_{\mathrm{RSI_B}}^2 + \sigma_{\mathrm{B}}^2} = \|\mathbf{h}_i^{\mathrm{B}}\|^2 \bar{\gamma}_{\mathrm{B}}, \quad (8)$$

where

$$\bar{\gamma}_{\mathrm{A}} = \frac{P_{\mathrm{B}}}{\sigma_{\mathrm{RSI_A}}^2 + \sigma_{\mathrm{A}}^2}, \text{ and } \bar{\gamma}_{\mathrm{B}} = \frac{P_{\mathrm{A}}}{\sigma_{\mathrm{RSI_B}}^2 + \sigma_{\mathrm{B}}^2}$$

are respectively the average SINR at transceiver A and B.

III. Performance Analysis

In this section, the system performance in terms of OP is analyzed using mathematical analysis. Since SINRs at A and B are similar, the expressions of OP at A and B are also similar. Therefore, to simplify presentation, we will provide only the detailed derivation of OP at one transceiver, e.g. B. The expression of A can be obtained by the same way.

At transceiver B, the OP is defined as follows [25]:

$$\mathcal{P}_{\mathrm{out}}^{\mathrm{B}} = \Pr\{\log_2(1 + \gamma_{\mathrm{B}}) < \mathcal{R}\}, \quad (9)$$

where $\gamma_{\rm B}$ is determined as in (8) and $\mathcal{R}$ is the normalized data rate of the transmission link from A to B. Replacing $\gamma_{\rm B}$ in (8) into (9), we have

$$\mathcal{P}_{\rm out}^{\rm B}=\Pr\{\gamma_{\rm B}<2^{\mathcal{R}}-1\}=\Pr\left\{\|\mathbf{h}_i^{\rm B}\|^2<\frac{2^{\mathcal{R}}-1}{\bar{\gamma}_{\rm B}}\right\}. \tag{10}$$

Given the threshold $\gamma_{\rm th}=2^{\mathcal{R}}-1$, the probability in (10) becomes

$$\mathcal{P}_{\rm out}^{\rm B}=\Pr\left\{\|\mathbf{h}_i^{\rm B}\|^2<\frac{\gamma_{\rm th}}{\bar{\gamma}_{\rm B}}\right\}. \tag{11}$$

From (11), we can obtain OP of the considered system using the following theorem.

Theorem: The OP expressions of the FD-SM-TAS system in the Rayleigh fading channels are calculated as follows:

$$\begin{aligned}\mathcal{P}_{\rm out}^{\rm A}=&\frac{\pi\gamma_{\rm th}}{2M(N_t^{\rm B}-w_{\rm B}+1)\Gamma(N_r^{\rm A})\bar{\gamma}_{\rm A}}\\&\times\sum_{l=w_{\rm B}}^{N_t^{\rm B}}\sum_{m=1}^{M}\frac{\sqrt{1-\phi_m^2}}{B(l,N_t^{\rm B}-l+1)}\left[1-\frac{\Gamma(N_r^{\rm A},\chi_{\rm A})}{\Gamma(N_r^{\rm A})}\right]^{l-1}\\&\times\left[\frac{\Gamma(N_r^{\rm A},\chi_{\rm A})}{\Gamma(N_r^{\rm A})}\right]^{N_t^{\rm B}-l}\chi_{\rm A}^{N_r^{\rm A}-1}e^{-\chi_{\rm A}},\end{aligned} \tag{12}$$

$$\begin{aligned}\mathcal{P}_{\rm out}^{\rm B}=&\frac{\pi\gamma_{\rm th}}{2M(N_t^{\rm A}-w_{\rm A}+1)\Gamma(N_r^{\rm B})\bar{\gamma}_{\rm B}}\\&\times\sum_{l=w_{\rm A}}^{N_t^{\rm A}}\sum_{m=1}^{M}\frac{\sqrt{1-\phi_m^2}}{B(l,N_t^{\rm A}-l+1)}\left[1-\frac{\Gamma(N_r^{\rm B},\chi_{\rm B})}{\Gamma(N_r^{\rm B})}\right]^{l-1}\\&\times\left[\frac{\Gamma(N_r^{\rm B},\chi_{\rm B})}{\Gamma(N_r^{\rm B})}\right]^{N_t^{\rm A}-l}\chi_{\rm B}^{N_r^{\rm B}-1}e^{-\chi_{\rm B}},\end{aligned} \tag{13}$$

where $\chi_{\rm A}=\frac{\gamma_{\rm th}}{2\bar{\gamma}_{\rm A}}(1+\phi_m);\chi_{\rm B}=\frac{\gamma_{\rm th}}{2\bar{\gamma}_{\rm B}}(1+\phi_m);w_{\rm A}=N_t^{\rm A}-S_{\rm A}+1;w_{\rm B}=N_t^{\rm B}-S_{\rm B}+1$; $B(.,.)$, $\Gamma(.)$ and $\Gamma(.,.)$ are the beta, gamma and incomplete gamma functions [26], respectively; M is the complexity-accuracy trade-off parameter; $\phi_m=\cos\left(\frac{(2m-1)\pi}{2M}\right)$.

Proof: To derive the OP expression at each transceiver A and B of the considered system, we start with the Cumulative Distribution Function (CDF) and the Probability Density Function (PDF) of one random instantaneous channel gain, i.e. $|h|^2$ which follows the Rayleigh distribution. The CDF and PDF of $|h|^2$ are given by

$$F_{|h|^2}(x)=\Pr\{|h|^2<x\}=1-e^{-\frac{x}{\Omega}},x\geqslant 0, \tag{14}$$

$$f_{|h|^2}(x)=\frac{1}{\Omega}e^{-\frac{x}{\Omega}},x\geqslant 0, \tag{15}$$

where $\Omega=\mathbb{E}\{|h|^2\}$ is the average channel gain of $|h|^2$. For presentation convenience and without loss of generality, let us set $\Omega=1$ in our further analysis. Denote the sum of $N_{\rm r}$ channel gains by $Y=\|\mathbf{h}_i^{\rm B}\|^2=\sum_{l=1}^{N_r^{\rm B}}|h_{il}|^2$, its PDF and CDF are computed by [4]:

$$F_Y(x)=1-e^{-x}\sum_{l=0}^{N_r^{\rm B}-1}\frac{x^l}{l!},\quad x\geq 0, \tag{16}$$

$$f_Y(x)=\frac{x^{N_r^{\rm B}-1}e^{-x}}{\Gamma(N_r^{\rm B})},\quad x\geq 0. \tag{17}$$

On the other hand, in the MIMO system with TAS, the set of the sum channel gains Y are arranged in a descending order and the first S antennas ($S_{\rm A}$ at transceiver A and $S_{\rm B}$ at transceiver B) are selected for transmission. At transceiver B, the PDF of $Y_{w_{\rm A}}^{\rm B}$ in the case that $Y_1^{\rm B}\leq Y_2^{\rm B}\leq\ ...\ \leq Y_{w_{\rm A}}^{\rm B}\leq\ ...\ \leq Y_{N_t^{\rm A}}^{\rm B}$ can be calculated as [27, Eq. 2.1.6]:

$$\begin{aligned}f_{Y_{w_{\rm A}}^{\rm B}}(x)=&\frac{1}{B(w_{\rm A},N_t^{\rm A}-w_{\rm A}+1)}\\&\times\Big[F_Y(x)\Big]^{w_{\rm A}-1}\Big[1-F_Y(x)\Big]^{N_t^{\rm A}-w_{\rm A}}f_Y(x).\end{aligned} \tag{18}$$

Based on this PDF, the PDF of the instantaneous channel gains $\|\mathbf{h}_i^{\rm B}\|^2$ is then given by [16]:

$$\begin{aligned}f_{\|\mathbf{h}_i^{\rm B}\|^2}(x)=&\frac{1}{N_t^{\rm A}-w_{\rm A}+1}\sum_{l=w_{\rm A}}^{N_t^{\rm A}}\frac{1}{B(l,N_t^{\rm A}-l+1)}\\&\times\Big[F_Y(x)\Big]^{l-1}\Big[1-F_Y(x)\Big]^{N_t^{\rm A}-l}f_Y(x).\end{aligned} \tag{19}$$

Replacing $F_Y(x)$ and $f_Y(x)$ in (16) and (17) into (19), we have

$$\begin{aligned}f_{\|\mathbf{h}_i^{\rm B}\|^2}(x)=&\frac{1}{N_t^{\rm A}-w_{\rm A}+1}\sum_{l=w_{\rm A}}^{N_t^{\rm A}}\frac{1}{B(l,N_t^{\rm A}-l+1)}\\&\times\left[1-e^{-x}\sum_{l=0}^{N_r^{\rm B}-1}\frac{x^l}{l!}\right]^{l-1}\left[e^{-x}\sum_{l=0}^{N_r^{\rm B}-1}\frac{x^l}{l!}\right]^{N_t^{\rm A}-l}\\&\times\frac{x^{N_r^{\rm B}-1}e^{-x}}{\Gamma(N_r^{\rm B})}.\end{aligned} \tag{20}$$

Applying the finite sums [26]

$$\sum_{l=0}^{N_r^{\rm B}-1}\frac{x^l}{l!}=e^x\frac{\Gamma(N_r^{\rm B},x)}{\Gamma(N_r^{\rm B})},$$

we can rewrite (20) as

$$\begin{aligned}f_{\|\mathbf{h}_i^{\rm B}\|^2}(x)=&\frac{1}{N_t^{\rm A}-w_{\rm A}+1}\sum_{l=w_{\rm A}}^{N_t^{\rm A}}\frac{1}{B(l,N_t^{\rm A}-l+1)}\\&\times\left[1-\frac{\Gamma(N_r^{\rm B},x)}{\Gamma(N_r^{\rm B})}\right]^{l-1}\left[\frac{\Gamma(N_r^{\rm B},x)}{\Gamma(N_r^{\rm B})}\right]^{N_t^{\rm A}-l}\\&\times\frac{x^{N_r^{\rm B}-1}e^{-x}}{\Gamma(N_r^{\rm B})}.\end{aligned} \tag{21}$$

Therefore, the OP at B is calculated as

$$\begin{aligned}\mathcal{P}_{\rm out}^{\rm B}=&\Pr\left\{\|\mathbf{h}_i^{\rm B}\|^2<\frac{\gamma_{\rm th}}{\bar{\gamma}_{\rm B}}\right\}=\int_0^{\frac{\gamma_{\rm th}}{\bar{\gamma}_{\rm B}}}f_{\|\mathbf{h}_i^{\rm B}\|^2}(x)dx\\=&\frac{1}{(N_t^{\rm A}-w_{\rm A}+1)\Gamma(N_r^{\rm B})}\sum_{l=w_{\rm A}}^{N_t^{\rm A}}\frac{1}{B(l,N_t^{\rm A}-l+1)}\\&\times\int_0^{\frac{\gamma_{\rm th}}{\bar{\gamma}_{\rm B}}}\left[1-\frac{\Gamma(N_r^{\rm B},x)}{\Gamma(N_r^{\rm B})}\right]^{l-1}\left[\frac{\Gamma(N_r^{\rm B},x)}{\Gamma(N_r^{\rm B})}\right]^{N_t^{\rm A}-l}\\&\times x^{N_r^{\rm B}-1}e^{-x}dx.\end{aligned} \tag{22}$$

Using the Gaussian-Chebyshev quadrature method in [28] for the integral in (22), we obtain the OP at transceiver B as in (13) in Theorem 1. The OP at transceiver A is derived in the same way.

The proof is complete.

It is also noted that, in the case without TAS, based on (16), the OP of the FD-SM system is given by

$$\mathcal{P}^{\mathrm{A}}_{\text{out,no-TAS}} = 1 - e^{-\frac{\gamma_{\mathrm{th}}}{\bar{\gamma}_{\mathrm{A}}}} \sum_{l=0}^{N_r^{\mathrm{A}}-1} \frac{\frac{\gamma_{\mathrm{th}}}{\bar{\gamma}_{\mathrm{A}}}}{l!}, \tag{23}$$

$$\mathcal{P}^{\mathrm{B}}_{\text{out,no-TAS}} = 1 - e^{-\frac{\gamma_{\mathrm{th}}}{\bar{\gamma}_{\mathrm{B}}}} \sum_{l=0}^{N_r^{\mathrm{B}}-1} \frac{\frac{\gamma_{\mathrm{th}}}{\bar{\gamma}_{\mathrm{B}}}}{l!}. \tag{24}$$

IV. Numerical Results and Discussions

In this section, we evaluate performance of the FD-SM-TAS system and compare it with the case without TAS. Moreover, performance of the HD-SM system is also investigated to understand the impact of the RSI on the FD-SM system. The parameters used for evaluation are chosen as follows: the average transmit power $P_A = P_B = P$, the number of transmit and receive antennas $N_t^{\mathrm{A}} = N_t^{\mathrm{B}} = N_t$ and $N_r^{\mathrm{A}} = N_r^{\mathrm{B}} = N_r$, the number of selected transmit antennas $S_{\mathrm{A}} = S_{\mathrm{B}} = S$, the variance of AWGN $\sigma_{\mathrm{A}}^2 = \sigma_{\mathrm{B}}^2 = \sigma^2 = 1$. With these parameters, the system becomes symmetrical leading to similar OPs at A and B. It is then sufficient to evaluate an arbitrary OP of transceiver A or B. Moreover, the average SNR is defined as $\mathrm{SNR} = P/\sigma^2$.

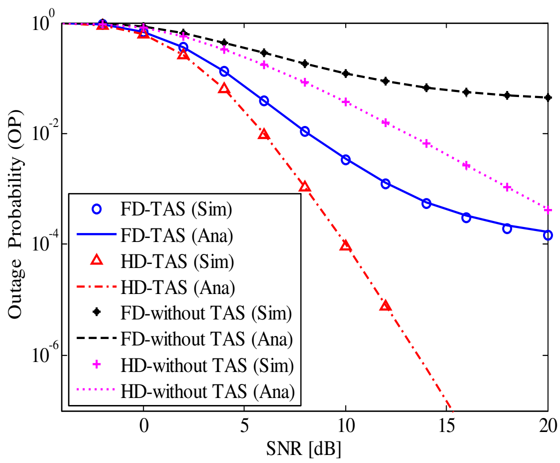

Figure 2. The OP performance of the FD-SM system with and without TAS versus the average SNR; $N_{\mathrm{r}} = 2, N_{\mathrm{t}} = 4, S = 2, \mathcal{R} = 2$ bit/s/Hz, $\tilde{\Omega} = -10$ dB.

In Fig. 2, we evaluate the OP of the FD-SM system with and without TAS in the case of $N_{\mathrm{r}} = 2, N_{\mathrm{t}} = 4, S = 2, \mathcal{R} = 2$ bit/s/Hz, $\tilde{\Omega} = -10$ dB. The OP of the HD-SM system is also shown for comparison. The OPs of the considered system with and without TAS are plotted by using (12) in Theorem and (23), respectively. Notice that the OPs of the HD-SM system are also used (12) and (23) after setting RSI to zero. As can be seen in the figure, the analytical curves match perfectly with the simulation ones, which validates Theorem 1. It is easily realized that using TAS significantly improves the OP performance of both FD-SM and HD-SM systems. When SNR $= 20$ dB, the OP of the FD-SM-TAS system drops to nearly 10^{-4} while the case without TAS, the OP is more than $4 \cdot 10^{-2}$. We also see that the OPs of the FD-SM systems suffer an outage floor due to the impact of RSI. With the considered RSI of $\tilde{\Omega} = -10$ dB, the OP of the FD-SM-TAS equals 6.10^{-4} at SNR $= 15$ dB while that of the HD-SM-TAS is 10^{-7}.

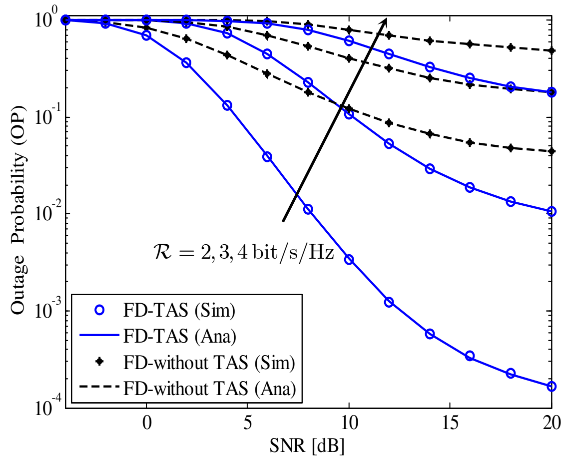

Figure 3. Impact of normalized transmission rate on the OP performance of the FD-SM system with and without TAS; $\mathcal{R} = 2, 3, 4$ bit/s/Hz, $N_r = 2, N_t = 4, S = 2, \tilde{\Omega} = -10$ dB.

Fig. 3 illustrates the impact of the normalized transmission rate $\mathcal{R}$ on the OP performance of the FD-SM system for $\mathcal{R} = 2, 3, 4$ bit/s/Hz. It is obvious that the transmission rate has a strong impact on the OP performance of the FD-SM system. At low transmission rate, i.e. $\mathcal{R} = 2$ bit/s/Hz, the OP of the system with TAS at SNR $= 12$ dB reduces to 10^{-3} while that of the case without TAS still equals 10^{-1}. The performance gap is thus 100 times. However, as the transmission rate increases, the OP curves of the system with TAS become saturated at high OP values, which reduces the performance gap between the case with and without TAS. For example, at $\mathcal{R} = 3$ bit/s/Hz and the same SNR, the performance gap reduces to only 10 times. Further increase to $\mathcal{R} = 4$ bit/s/Hz results in a gap of only 3 times. This reduction tendency reflects the significant impact of the transmission rate on the system performance.

Fig. 4 illustrates the impact of RSI on the OP performance of the FD-SM system for $\tilde{\Omega} = 0, -5, -10, -20$ dB. It is obvious that the RSI has a strong impact on the OP performance of the FD-SM systems with and without TAS, especially for large RSI. When RSI is very small, e.g $\tilde{\Omega} = -20$ dB, the OPs of the FD-SM and HD-SM systems with TAS are similar at SNR < 10 dB. At higher SNR, i.e. SNR > 10 dB, the OP performance of the FD-SM-TAS system is lower than that of the HD-SM-TAS. Since RSI is expressed as $\sigma_{\mathrm{RSI}}^2 = \tilde{\Omega} P$, the RSI level increases for higher transmit power levels and this is the reason that the impact of RSI is stronger at high SNR regime. In the case without TAS, the difference between the OPs of the FD-SM and HD-SM systems become significant for SNR > 14 dB when $\tilde{\Omega} = -20$ dB. For larger RSI, i.e. $\tilde{\Omega} = -5$ dB or $\tilde{\Omega} = 0$ dB, the OPs of the FD-SM system

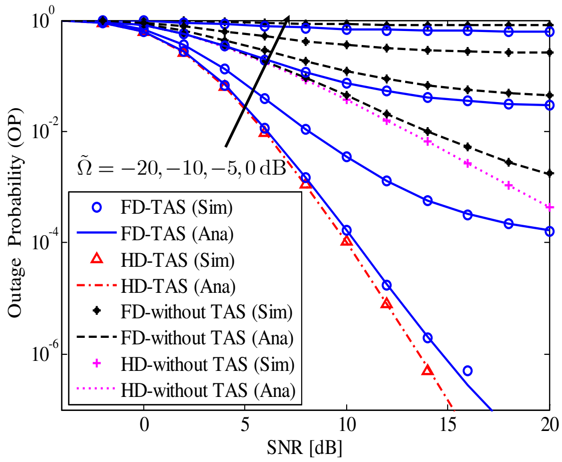

Figure 4. Impact of RSI on the OP performance of FD-SM system with and without TAS in the case of $N_{\mathrm{r}} = 2, N_{\mathrm{t}} = 4, S = 2, \mathcal{R} = 2$ bit/s/Hz.

become saturated soon for both the cases with and without TAS.

V. Conclusion

FD-SM technique is a promising transmission solution for MIMO wireless communications, especially in the era of scarce frequency spectrum. However, there are two important factors that strongly influence the system performance, i.e. the SI level which depends on the SIC capability and the normalized transmission rate which varies with the applications. In this paper, we have demonstrated that using TAS can help to improve the OP performance of the system and thus can lessen the impact of SI. However, TAS is more effective for low level of RSI and low transmission rate. Considering the tradeoff between performance improvement and the system complexity, it is recommended that the application of TAS is used only for a system with low normalized transmission rate and high SIC capability.

References

[1] Z. Zhang, X. Chai, K. Long, A. V. Vasilakos, and L. Hanzo, "Full duplex techniques for 5g networks: self-interference cancellation, protocol design, and relay selection," *IEEE Commununications Magazine*, vol. 53, no. 5, pp. 128–137, May 2015.

[2] B. Jiao, M. Wen, M. Ma, and H. V. Poor, "Spatial modulated full duplex," *IEEE Wireless Communications Letters*, vol. 3, no. 6, p. 641644, 2014.

[3] X. N. Tran, B. C. Nguyen, and D. T. Tran, "Outage probability of two-way full-duplex relay system with hardware impairments," in *2019 3rd International Conference on Recent Advances in Signal Processing, Telecommunications & Computing (SigTelCom)*. IEEE, 2019, pp. 135–139.

[4] B. C. Nguyen, T. M. Hoang, and P. T. Tran, "Performance analysis of full-duplex decode-and-forward relay system with energy harvesting over nakagami-m fading channels," *AEU-International Journal of Electronics and Communications*, vol. 98, pp. 114–122, 2019.

[5] B. C. Nguyen, X. N. Tran, and D. T. Tran, "Performance analysis of in-band full-duplex amplify-and-forward relay system with direct link," in *Recent Advances in Signal Processing, Telecommunications & Computing (SigTelCom), 2018 2nd International Conference on*. IEEE, 2018, pp. 192–197.

[6] B. C. Nguyen and T. M. Hoang, "Performance analysis of vehicle-to-vehicle communication with full-duplex amplify-and-forward relay over double-rayleigh fading channels," *Vehicular Communications*, p. 100166, 2019.

[7] X. N. Tran, T. M. Hoang, and N. B. Cao, "Outage performance of the downlink noma relay networks with rf energy harvesting and buffer aided relay," in *International Conference on Industrial Networks and Intelligent Systems*. Springer, Conference Proceedings, pp. 164–177.

[8] B. C. Nguyen and X. N. Tran, "Performance analysis of full-duplex amplify-and-forward relay system with hardware impairments and imperfect self-interference cancellation," *Wireless Communications and Mobile Computing*, vol. 2019, p. 10, 2019. [Online]. Available: https://doi.org/10.1155/2019/4946298

[9] B. C. Nguyen, T. M. Hoang, and S.-G. Choi, "Full-duplex relay system with energy harvesting: Outage and symbol error probabilities," in *2018 International Conference on Advanced Technologies for Communications (ATC)*. IEEE, Conference Proceedings, pp. 360–365.

[10] Z. Wei, X. Zhu, S. Sun, Y. Jiang, A. Al-Tahmeesschi, and M. Yue, "Research issues, challenges, and opportunities of wireless power transfer-aided full-duplex relay systems," *IEEE Access*, vol. 6, pp. 8870–8881, 2018.

[11] M. Le, V. Ngo, H. Mai, X. N. Tran, and M. D. Renzo, "Spatially modulated orthogonal space-time block codes with non-vanishing de-terminants," *IEEE Transactions on Communications*, vol. 62, no. 1, p. 8599, 2014.

[12] T. P. Nguyen, M. T. Le, V. D. Ngo, X. N. Tran, and H. W. Choi, "Spatial modulation for high-rate transmission systems," in *2014 IEEE 79th Vehicular Technology Conference (VTC Spring)*. IEEE, 2014.

[13] J. Zhang, Q. Li, K. J. Kim, Y. Wang, X. Ge, and J. Zhang, "On the performance of full-duplex two-way relay channels with spatial modulation," *IEEE Transactions on Communications*, vol. 64, no. 12, p. 49664982, 2016.

[14] A. Koc, I. Altunbas, and E. Basar, "Full-duplex spatial modulation systems under imperfect channel state information," in *2017 24th International Conference on Telecommunications (ICT)*. IEEE, 2017.

[15] S. Narayanan, H. Ahmadi, and M. F. Flanagan, "On the performance of spatial modulation mimo for full-duplex relay networks," *IEEE Transactions on Wireless Communications*, vol. 16, no. 6, p. 37273746, 2017.

[16] B. Kumbhani and R. Kshetrimayum, "Outage probability analysis of spatial modulation systems with antenna selection," *Electronics Letters*, vol. 50, no. 2, pp. 125–126, 2014.

[17] P. Yang, Y. Xiao, Y. L. Guan, S. Li, and L. Hanzo, "Transmit antenna selection for multiple-input multiple-output spatial modulation systems," *IEEE Transactions on Communications*, vol. 64, no. 5, pp. 2035–2048, 2016.

[18] X. Wu, M. D. Renzo, and H. Haas, "Adaptive selection of antennas for optimum transmission in spatial modulation," *IEEE Transactions on Wireless Communications*, vol. 14, no. 7, pp. 3630–3641, 2015.

[19] S. Jang, M. Ahn, H. Lee, and I. Lee, "Antenna selection schemes in bidirectional full-duplex mimo systems," *IEEE Transactions on Vehicular Tecnology*, vol. 65, no. 12, p. 1009710100, 2016.

[20] E. Fidan and O. Kucur, "Performance of transceiver antenna selection in two way full-duplex relay networks over rayleigh fading channels," *IEEE Transactions on Vehicular Technology*, vol. 67, no. 7, pp. 5909–5921, 2018.

[21] M. Zhou, H. Cui, L. Song, and B. Jiao, "Transmit-receive antenna pair selection in full duplex systems," *IEEE Wireless Communications Letter*, vol. 3, Number = 1, Publisher = IEEE,, pp. 34–37, 2014.

[22] T. Riihonen, S. Werner, and R. Wichman, "Mitigation of loopback self-interference in full-duplex mimo relays," *IEEE Transactions on Signal Processing*, vol. 59, no. 12, pp. 5983–5993, 2011.

[23] E. Aryafar, M. A. Khojastepour, K. Sundaresan, S. Rangarajan, and M. Chiang, "Midu: Enabling mimo full duplex," in *Proceedings of the 18th annual international conference on Mobile computing and networking*. ACM, 2012, pp. 257–268.

[24] C. Li, Z. Chen, Y. Wang, Y. Yao, and B. Xia, "Outage analysis of the full-duplex decode-and-forward two-way relay system," *IEEE Transactions on Vehicular Technology*, vol. 66, no. 5, pp. 4073–4086, May 2017.

[25] A. Goldsmith, *Wireless communications*. Cambridge university press, 2005.

[26] A. Jeffrey and D. Zwillinger, *Table of integrals, series, and products*. Academic press, 2007.

[27] H. A. David and H. N. Nagaraja, "Order statistics," *Encyclopedia of Statistical Sciences*, 2004.

[28] M. Abramowitz and I. A. Stegun, *Handbook of mathematical functions with formulas, graphs, and mathematical tables*. Dover, New York, 1972, vol. 9.